In higher-latitude areas, particularly in the Northern Hemisphere, there are significant temperature changes that do not appear to be directly related to land-cover change. Although statistically significant, these changes are relatively small as compared to the projected atmospheric forcing changes. For example, in western Russia there is reforestation in both scenarios, which should lead to warming. However, although the additional land-cover changes have the expected impact on net radiation, the B1 and A2 scenarios show strongly opposing temperature signals in December, January, and February (DJF). These results appear to be closely linked to changes in regional precipitation and may be the result of teleconnections, either linked to the Asian Monsoon circulation or indirect effects from temperature changes over the tropical Pacific and North Atlantic Oceans.

Results from this study suggest that the choices humans make about future land use could have a significant impact on regional and seasonal climates. Some of these effects are the result of direct impacts of land-cover change on local moisture and energy balances. Other impacts appear to be related to significant indirect climate effects through teleconnection processes. The A2 land-cover scenario shows that tropical rainforest conversion will likely lead to a weakening of the Hadley circulation over much of the world and to significant changes in the Asian Monsoon circulation. Especially in the A2 2050 scenario, the interplay between Asian and African land-cover change affects the Asian Monsoon circulation. The Indian Ocean experiences a significant reduction in surface pressure, resulting in increased cloud cover and precipitation and warmer surface temperatures, and these effects extend over most of the Indian subcontinent.

We conclude that the inclusion of land-cover forcing, thereby accounting for a number of additional anthropogenic climate impacts, will improve the quality of regional climate assessments for IPCC SRES scenarios. Although land-cover effects are regional and tend to offset with respect to global average temperatures, they can significantly alter regional climate outcomes associated with global warming. Beyond local impacts, tropical land-cover change can potentially affect extratropical climates and nearby ocean conditions through atmospheric teleconnections. In this respect, our fully coupled experiments differ from previous fixed ocean temperature studies (*12*, *13*, *15*). Further study is needed to determine the exact nature of these responses. Overall, the results demonstrate the importance of including land-cover change in forcing scenarios for future climate change studies.

References and Notes

1. J. J. Houghton *et al.*, Eds., *Climate Change 2000: The Scientific Basis* (IPCC Working Group I, Cambridge Univ. Press, Cambridge, 2001).
2. P. Kabat *et al.*, *Vegetation, Water, Humans and the Climate Change: A New Perspective on an Interactive System* (Springer, Heidelberg, Germany, 2002).
3. W. Steffen *et al.*, *Global Change and the Earth System: A Planet Under Pressure* (Springer-Verlag, New York, 2004).
4. R. A. Betts, *Atmos. Sci. Lett.* **2**, 39 (2001).
5. L. R. Bounoua, R. DeFries, G. J. Collatz, P. Sellers, H. Khan, *Clim. Change* **52**, 29 (2002).
6. T. N. Chase, R. A. Peilke Sr., T. G. F. Kittel, R. R. Nemani, S. W. Running, *Clim. Dyn.* **16**, 93 (2000).
7. J. J. Feddema *et al.*, *Clim. Dyn.* **25**, 581 (2005).
8. J. Hansen *et al.*, *Proc. Natl. Acad. Sci. U.S.A.* **95**, 12753 (1998).
9. H. D. Matthews, A. J. Weaver, K. J. Meissner, N. P. Gillett, M. Eby, *Clim. Dyn.* **22**, 461 (2004).
10. M. H. Costa, J. A. Foley, *J. Clim.* **13**, 18 (2000).
11. N. Gedney, P. J. Valdes, *Geophys. Res. Lett.* **27**, 3053 (2000).
12. K. McGuffie, A. Henderson-Sellers, H. Zhang, T. B. Durbidge, A. J. Pitman, *Global Planet. Change* **10**, 97 (1995).
13. R. S. DeFries, L. Bounoua, G. J. Collatz, *Global Change Biol.* **8**, 438 (2002).
14. S. Sitch *et al.*, *Global Biogeochem. Cycles* **19**, GB2013 (2004).
15. R. Avissar, D. Werth, *J. Hydrometeorol.* **6**, 134 (2005).
16. R. A. Pielke Sr. *et al.*, *Philos. Trans. R. Soc. London Ser. A* **360**, 1705 (2002).
17. G. Krinner *et al.*, *Global Biogeochem. Cycles* **19**, GB1015 (2005).
18. P. K. Snyder, C. Delire, J. A. Foley, *Clim. Dyn.* **23**, 279 (2004).
19. G. B. Bonan, D. Pollard, S. L. Thompson, *Nature* **359**, 716 (1992).
20. G. A. Meehl *et al.*, *Science* **307**, 1769 (2005).
21. W. M. Washington *et al.*, *Clim. Dyn.* **16**, 755 (2000).
22. N. Nakićenović *et al.*, *Special Report on Emissions Scenarios* (Cambridge Univ. Press, Cambridge, 2000).
23. J. Alcamo, R. Leemans, E. Kreileman, Eds., *Global Change Scenarios of the 21st Century. Results from the IMAGE 2.1 Model* (Pergamon Elsevier Science, London, 1998).
24. IMAGE 2.2 CD release and documentation (Rijks Instituut voor Volksgezondheid en Milieu, Bilthoven, Netherlands, 2002). The IMAGE 2.2 implementation of the SRES scenarios: *A Comprehensive Analysis of Emissions, Climate Change and Impacts in the 21st Century* (see www.rivm.nl/image/index.html for further information).
25. Materials and methods are available as supporting material on *Science* Online.
26. T. R. Karl, R. W. Knight, *Bull. Am. Meteorol. Soc.* **78**, 1107 (1997).
27. M. P. Hoerling, J. W. Hurrell, T. Xu, G. T. Bates, A. S. Phillips, *Clim. Dyn.* **23**, 391 (2004).
28. G. B. Bonan, *Ecol. Appl.* **9**, 1305 (1999).
29. G. B. Bonan, *J. Clim.* **14**, 2430 (2001).

30. We acknowledge the large number of scientists who have assisted in the development of the models and tools used to create the simulations used in this study. Special thanks to A. Middleton, T. Bettge, and G. Strand for their assistance in running the model and assistance with data processing and to R. Leemans for providing the SRES data. This research was supported by the Office of Science (Biological and Environmental Research Program), U.S. Department of Energy, under Cooperative Agreement No. DE-FC02-97ER62402; NSF (grant numbers ATM-0107404 and ATM-0413540); the National Center for Atmospheric Research Weather and Climate Impact Assessment Science Initiative supported by NSF; and the Center for Research, University of Kansas, Lawrence, KS.

Supporting Online Material

www.sciencemag.org/cgi/content/full/310/5754/1674/DC1
Materials and Methods
Figs. S1 and S2
References

29 July 2005; accepted 25 October 2005
10.1126/science.1118160

Equivalent Effects of Snake PLA2 Neurotoxins and Lysophospholipid–Fatty Acid Mixtures

Michela Rigoni,[1] Paola Caccin,[1] Steve Gschmeissner,[2] Grielof Koster,[3] Anthony D. Postle,[3] Ornella Rossetto,[1] Giampietro Schiavo,[2] Cesare Montecucco[1]*

Snake presynaptic phospholipase A2 neurotoxins (SPANs) paralyze the neuromuscular junction (NMJ). Upon intoxication, the NMJ enlarges and has a reduced content of synaptic vesicles, and primary neuronal cultures show synaptic swelling with surface exposure of the lumenal domain of the synaptic vesicle protein synaptotagmin I. Concomitantly, these neurotoxins induce exocytosis of neurotransmitters. We found that an equimolar mixture of lysophospholipids and fatty acids closely mimics all of the biological effects of SPANs. These results draw attention to the possible role of local lipid changes in synaptic vesicle release and provide new tools for the study of exocytosis.

SPANs are major protein components of the venom of many snakes (*1*–*3*). They block the NMJ in a characteristic way (*3*–*7*). The phospholipase A2 (PLA2) activity varies greatly among different SPANs, and its involvement in the NMJ block is still debated (*3*, *8*, *9*). There is only a partial correlation between PLA2 activity and neurotoxicity among SPANs and no overlap of surface residues required for neurotoxicity with those essential for PLA2 activity (*8*, *10*). Here, we compared the effects of SPANs on the mouse NMJ hemidiaphragm preparation and on neurons in culture with those of their hydrolysis products: lysophospholipids (LysoPL) and fatty acids (FAs). To conclusive-

[1]Department of Biomedical Sciences and Consiglio Nazionale Ricerche Institute of Neuroscience, University of Padova, Italy. [2]Cancer Research UK, London Research Institute, London, UK. [3]School of Medicine, University of Southampton, UK.

*To whom correspondence should be addressed. E-mail: cesare.montecucco@unipd.it

ly determine the nature of SPAN hydrolysis products, cerebellar neurons were treated with SPANs, and their lipid composition was determined by mass spectrometry. The major hydrolytic substrate was phosphatidylcholine, the main phospholipid of the outer leaflet of the plasma membrane (fig. S1). SPAN hydrolysis generated several lysophosphatidylcholines (LysoPC), including myristoyl lysophosphatidylcholine (mLysoPC), and FA. SPANs were not selective for a particular FA species (such as arachidonic acid) and released mainly oleic acid (OA), the most abundant FA of these cells.

The incubation of cerebellar neurons with mLysoPC+OA (30 μM each) led to the incorporation of 6.3 nmol of mLysoPC/10^5 cells, compared with 2.3 nmol/10^5 cells treated with 6 nM taipoxin. mLysoPC+OA did not cause acylation, because the 14.0 to 16.0 ratio in PC did not increase. The values of LysoPC associated with neurons in the two cases were closely comparable, particularly if one considers that SPANs induce a localized release of LysoPL and FA, whereas the incubation with mLysoPC+OA presumably caused generalized lipid insertion.

mLysoPC+OA added to a mouse hemidiaphragm in a physiological medium caused a progressive NMJ paralysis with a time course superimposable to that observed with a typical SPAN (Fig. 1A). Four SPANs of different structural complexity and relative toxicity were used: the single-chain notexin (14 kD, from *Notechis scutatus*), the two-subunit β-bungarotoxin (21 kD, from *Bungarus multicinctus*), the three-subunit taipoxin (42 kD, from *Oxyuranus scutellatus*), and the five-subunit textilotoxin (72 kD, from *Pseudonaja textilis*) (*1*). They induced closely similar paralysis profiles, although with slightly different kinetics; one representative trace is shown. When textilotoxin and mLysoPC+OA were present at the same time (1.5 nM and 50 μM, respectively), a synergistic effect was observed, with the time required to achieve 50% of paralysis ($t_{1/2}$) shorter by a factor of 4 ± 0.5 times (n = 4) than that of textilotoxin. Pancreatic PLA2 (at a concentration matching the activity of textilotoxin in Fig. 1A) did paralyze the NMJ, but with a $t_{1/2}$ three times as long, presumably because of a reduced membrane interaction.

Of the two products of SPAN phospholipid hydrolysis, LysoPC alone was capable of inhibiting the NMJ, although with low potency, whereas FA was poorly effective below the threshold concentration inducing myotoxicity; however, FA and LysoPC clearly acted synergistically (Fig. 1B).

Similar results were obtained with other LysoPL, such as the ethanolamine, serine, and glycerol derivatives. We also tested the effect of LysoPC esterified with FAs of different length and saturation obtaining similar results, but different kinetics, with the following order of $t_{1/2}$: myristoyl-LysoPC (taken as 1, to normalize the data obtained in five different experiments), oleoyl-LysoPC (2.2 ± 0.5 times as long), palmitoyl-LysoPC (3.2 ± 1.3), and stearoyl-LysoPC (8.5 ± 0.6). Their potency correlates with their critical micellar concentrations (*11*, *12*), indicating that the more water-soluble LysoPC equilibrates more rapidly into the membrane and acts faster; it is also possible that the shorter LysoPL causes a higher constraint on the membrane curvature. The paralysis was not due to an effect of mLysoPC+OA on the muscle itself, because direct muscle stimulation elicited full contraction and the muscle maintained its normal ultrastructure (Fig. 1, C and D). The mLysoPC+OA mixture induced diagnostic alterations in the ultrastructure of the NMJ, including a reduction of the number of synaptic vesicles and an enlargement of the nerve terminal (Fig. 1C), which closely mimic the changes observed in SPAN-treated NMJs (*4*–*7*).

SPANs induced a characteristic swelling of synaptic boutons in cultured neurons, with depletion of synaptic vesicles, release of glutamate and FM1-43, and surface exposure of the intralumenal portion of the synaptic vesicle protein synaptotagmin I (SytI) (*13*, *14*). Similarly to SPANs, mLysoPC+OA induced bulges (Fig. 2A) that were strongly stained by an antibody specific for the lumenal domain of SytI in the absence of membrane permeabilization, indicating a persistent surface exposure of the inside of synaptic vesicles (Fig. 2B). Control experiments showed no labeling with an antibody specific for a cytosolic SytI epitope, indicating that the mLysoPC+OA mixture did not permeabilize the neuronal membrane. Bulges were also stained by an antibody specific for synaptophysin I, a marker of synaptic vesicles, showing that they are sites of synaptic vesicle accumulation (fig. S2). Concomitantly to bulge formation, mLysoPC+OA induced neurons to release glutamate as SPANs did (respectively, 92 ± 1% and 78 ± 1% of the amount released upon incubation with 55 mM KCl, taken as 100%; n = 5). Thus, mLysoPC+OA acts at nerve terminals in a manner identical, or superimposable, to that of SPANs.

The biological action of SPANs at nerve terminals can now be rationalized as follows: SPANs bind nerve terminals via receptors whose nature may differ for different SPANs (*1*–*3*), gaining access to membrane phospholipids that are hydrolyzed to LysoPL and FA. LysoPL remain confined mainly to the external leaflet of the presynaptic membrane, whereas FAs have a high rate of transbilayer movement (*15*) and will partition between the two membrane leaflets. Such configuration, with the inverted cone-shaped LysoPL in *trans* and the cone-shaped FA in *cis,* with respect to the membrane fusion site, promotes the fusion-through-hemifusion pathway (*16*, *17*). This would promote neurotransmitter release (*13*, *14*). Hemifusion lipid intermediates have been recently observed in the SNARE-mediated membrane fusion (*18*–*20*). A local change of lipid composition within the site of assembly of the SNARE complex has been suggested to promote the fusion of synaptic vesicles with the presynaptic membrane (*21*–*23*), and there is evidence for the involve-

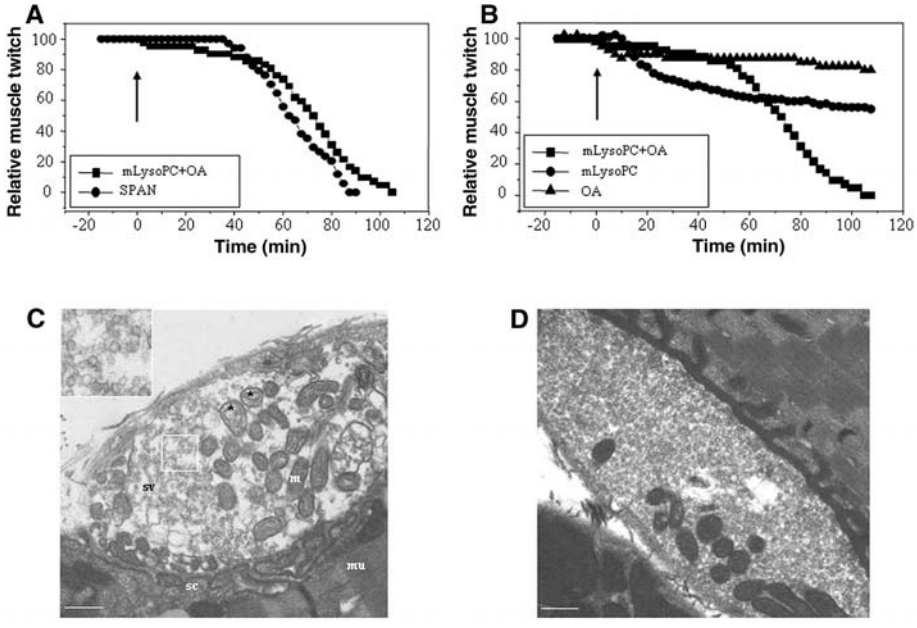

Fig. 1. Paralysis induced by mLysoPC+OA (bath concentration 150 μM) or textilotoxin (15 nM) added (arrows) to the medium of mouse phrenic nerve-hemidiaphragm (**A**). Similar curves were obtained with other SPANs (notexin, β-bungarotoxin, and taipoxin) and other lipid mixtures. (**B**) Activity of the lipid species (150 μM) alone or together. Representative traces are shown in (A) and (B) ($n \geq 5$). (**C**) Representative electron micrographs of a mouse hemidiaphragm paralyzed with mLysoPC+OA (150 μM) and of the corresponding contralateral muscle (**D**). mu, muscle; sc, synaptic cleft; sv, synaptic vesicles. The inset shows an enlarged area containing sv; asterisks indicate swollen mitochondria (m). Scale bar, 0.5 μm.

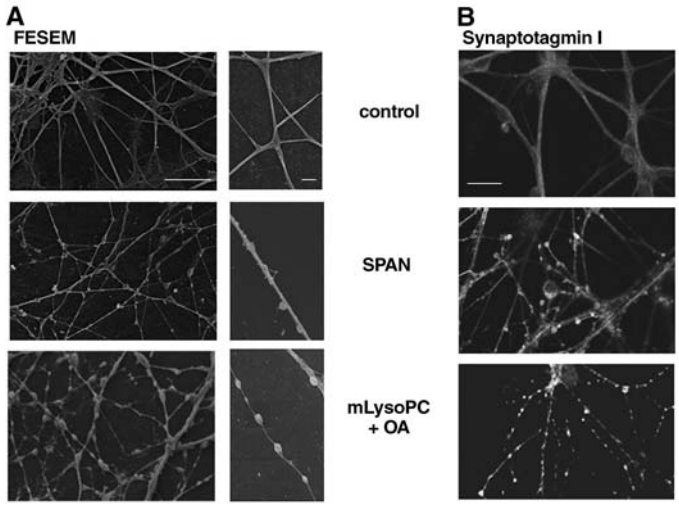

Fig. 2. Field emission scanning electron microscopy (FESEM) of cerebellar granular neurons exposed to taipoxin (6 nM for 60 min) or mLysoPC+OA (30 μM for 15 min) at lower (left panels) and higher (right panels) magnifications (**A**). Identical results were obtained with notexin, β-bungarotoxin, and textilotoxin. Scale bar, 10 μm (left panels) and 2 μm (right panels). (**B**) Cerebellar neurons were exposed to 6 nM β-bungarotoxin for 60 min or to 30 μM mLysoPC+OA for 15 min and stained with an antibody specific for the lumenal domain of synaptotagmin I before fixation. Samples were processed for indirect immunofluorescence without permeabilization; superimposable results were obtained with notexin, taipoxin, and textilotoxin in cerebellar neurons and hippocampal neurons. Scale bar, 10 μm.

ment of PLA2 in other exocytotic events such as the sperm acrosomal exocytosis (*24*). Furthermore, a SPAN microinjected into pheochromocytoma cells inhibited neuroexocytosis (*25*), presumably because it acted on the cytosolic plasma membrane side, inducing an opposite membrane configuration. The presence of clathrin-coated Ω-shaped structures in SPAN-poisoned NMJs (*4*–*7*) suggested that they also inhibit synaptic vesicle fission from the plasma membrane (*3*, *14*). Indeed, the same SPAN-induced lipid changes promoting membrane fusion do inhibit membrane fission for the same physical and topological reasons (*17*).

References and Notes

1. R. M. Kini, Ed., *Venom Phospholipase A2 Enzymes* (Wiley, Chichester, UK, 1997).
2. G. Schiavo, M. Matteoli, C. Montecucco, *Physiol. Rev.* **80**, 717 (2000).
3. C. Montecucco, O. Rossetto, *Trends Biochem. Sci.* **25**, 266 (2000).
4. S. G. Cull-Candy, J. Fohlman, D. Gustavsson, R. Lullmann-Rauch, S. Thesleff, *Neuroscience* **1**, 175 (1976).
5. I. L. Chen, C. Y. Lee, *Virchows Arch. B Cell Pathol.* **6**, 318 (1970).
6. J. B. Harris, B. D. Grubb, C. A. Maltin, R. Dixon, *Exp. Neurol.* **161**, 517 (2000).
7. C. Y. Lee, M. C. Tsa, Y. M. Chen, A. Ritonja, F. Gubensek, *Arch. Int. Pharmacodyn. Ther.* **268**, 313 (1984).
8. P. Rosenberg, *Venom Phospholipase A2 Enzymes*, R. M. Kini, Ed. (Wiley, Chichester, UK, 1997), pp. 155-183.
9. R. M. Kini, *Toxicon* **42**, 827 (2003).
10. C. C. Yang, in *Venom Phospholipase A2 Enzymes*, R. M. Kini, Ed. (Wiley, Chichester, UK,1997), pp. 185-204.
11. R. E. Stafford, T. Fanni, E. A. Dennis, *Biochemistry* **28**, 5113 (1989).
12. J. Wang *et al.*, *Br. J. Pharmacol.* **141**, 586 (2004).
13. M. Rigoni *et al.*, *J. Cell Sci.* **15**, 3561 (2004).
14. D. Bonanomi *et al.*, *Mol. Pharmacol.* **67**, 1901 (2005).
15. F. Kamp, D. Zakim, F. Zhang, N. Noy, J. A. Hamilton, *Biochemistry* **34**, 11928 (1995).
16. L. V. Chernomordik, E. Leikina, V. Frolov, P. Bronk, J. Zimmerberg, *J. Cell Biol.* **136**, 81 (1997).
17. L. V. Chernomordik, M. M. Kozlov, *Annu. Rev. Biochem.* **72**, 175 (2003).
18. Y. Xu, F. Zhang, Z. Su, J. A. McNew, Y. K. Shin, *Nat. Struct. Mol. Biol.* **12**, 417 (2005).
19. C. G. Giraudo *et al.*, *J. Cell Biol.* **170**, 249 (2005).
20. C. Reese, F. Heise, A. Mayer, *Nature* **436**, 410 (2005).
21. K. Farsad, P. De Camilli, *Curr. Opin. Cell Biol.* **15**, 372 (2003).
22. R. Jahn, T. Lang, T. C. Sudhof, *Cell* **112**, 519 (2003).
23. L. K. Tamm, J. Crane, V. Kiessling, *Curr. Opin. Struct. Biol.* **13**, 453 (2003).
24. E. R. S. Roldan, *Front. Biosci.* **3**, 1119 (1998).
25. S. Wei *et al.*, *Neuroscience* **121**, 891 (2003).
26. Supported by Telethon grant GP0272Y01, COFIN Project 2002055747, FISR-DM 16/10/00, FIRB-RBNE01RHZM, University of Padova, and Cancer Research UK.

Supporting Online Material

www.sciencemag.org/cgi/content/full/310/5754/1678/DC1
Materials and Methods
Figs. S1 and S2
References

27 September 2005; accepted 4 November 2005
10.1126/science.1120640

Neural Systems Responding to Degrees of Uncertainty in Human Decision-Making

Ming Hsu,[1] Meghana Bhatt,[1] Ralph Adolphs,[1,2] Daniel Tranel,[2] Colin F. Camerer[1]*

Much is known about how people make decisions under varying levels of probability (risk). Less is known about the neural basis of decision-making when probabilities are uncertain because of missing information (ambiguity). In decision theory, ambiguity about probabilities should not affect choices. Using functional brain imaging, we show that the level of ambiguity in choices correlates positively with activation in the amygdala and orbitofrontal cortex, and negatively with a striatal system. Moreover, striatal activity correlates positively with expected reward. Neurological subjects with orbitofrontal lesions were insensitive to the level of ambiguity and risk in behavioral choices. These data suggest a general neural circuit responding to degrees of uncertainty, contrary to decision theory.

In theories of choice under uncertainty used in social sciences and behavioral ecology, the only variables that should influence an uncertain choice are the judged probabilities of possible outcomes and the evaluation of those outcomes. But confidence in judged probability can vary widely. In some choices, such as gambling on a roulette wheel, probability can be confidently judged from relative frequencies, event histories, or an accepted theory. At the other extreme, such as the chance of a terrorist attack, probabilities are based on meager or conflicting evidence, where important information is clearly missing. The two types of uncertain events are often called risky and ambiguous, respectively. In subjective expected utility theory, the probabilities of outcomes should influence choices, whereas confidence about those probabilities should not. But experiments show that many people are more willing to bet on risky outcomes than on ambiguous ones, holding judged probability of outcomes constant (*1*). This empirical aversion to ambiguity motivates a search for neural distinctions between risk and ambiguity. Here, we extend the study of the neural basis of decision under risk to encompass ambiguity.

The difference between risky and ambiguous uncertainty is illustrated by the Ellsberg paradox (*2*). Imagine one deck of 20 cards composed of 10 red and 10 blue cards (the risky deck). Another deck has 20 red or blue cards, but the composition of red and blue cards is completely unknown (the ambiguous deck). A bet on a color pays a fixed sum (e.g., $10) if a card with the chosen color is drawn, and zero otherwise (Fig. 1A).

[1]Division of Humanities and Social Sciences, 228-77, California Institute of Technology, Pasadena, CA 91125, USA. [2]University of Iowa Medical School, Iowa City, IA 52242, USA.

*To whom correspondence should be addressed. E-mail: camerer@hss.caltech.edu

Equivalent Effects of Snake PLA2 Neurotoxins and Lysophospholipid-Fatty Acid Mixtures

Michela Rigoni *et al.*

Science **310**, 1678 (2005);
DOI: 10.1126/science.1120640

Science (print ISSN 0036-8075; online ISSN 1095-9203) is published weekly, except the last week in December, by the American Association for the Advancement of Science, 1200 New York Avenue NW, Washington, DC 20005.